



Research article

Cascaded robust control of mechanical ventilator using fractional order sliding mode control

Nasim Ullah* and Al-sharef Mohammad

Department of Electrical Engineering College of Engineering, TAIF University, TAIF 11099, Saudi Arabia

* **Correspondence:** Email: nasimullah@tu.edu.sa.

Abstract: A mechanical ventilator is an important medical equipment that assists patients who have breathing difficulties. In recent times a huge percentage of COVID-19 infected patients suffered from respiratory system failure. In order to ensure the abundant availability of mechanical ventilators during COVID-19 pandemic, most of the manufacturers around the globe utilized open source designs. Patients safety is of utmost importance while using mechanical ventilators for assisting them in breathing. Closed loop feedback control system plays vital role in ensuring the stability and reliability of dynamical systems such as mechanical ventilators. Ideal characteristics of mechanical ventilators include safety of patients, reliability, quick and smooth air pressure buildup and release. Unfortunately most of the open source designs and mechanical ventilator units with classical control loops cannot achieve the above mentioned ideal characteristics under system uncertainties. This article proposes a cascaded approach to formulate robust control system for regulating the states of ventilator unit using blower model reduction techniques. Model reduction allows to cascade the blower dynamics in the main controller design for airway pressure. The proposed controller is derived based on both integer and non integer calculus and the stability of the closed loop is ensured using Lyapunov theorems. The effectiveness of the proposed control method is demonstrated using extensive numerical simulations.

Keywords: mechanical ventilator; COVID-19; non integer control; robust control; sliding mode control

1. Introduction

In recent times WHO declared a worldwide pandemic due to emergence of a novel corona virus in 2019 (COVID-19) and as per WHO several millions people are tested positive to date. Since the number of infected population due to COVID-19 is several millions, so in spite of low fatality rate, around 2 million infected people died. Such massive number of deaths are reported because as per

an estimate 40 percent of the total infected people showed respiratory system failure [1]. Critical patients with partial failure of their respiratory system require mechanical ventilation for assisting them in breathing. The mechanical ventilators are being utilized since 18th century as open loop devices, however the first closed loop mechanical ventilator was reported in 1950. In mass emergency situations due to COVID-19, Massachusetts Institute of Technology (MIT) played a crucial and leading role by developing a MIT emergency ventilator project and the design and specifications of such ventilator units are placed as open source material [2]. MIT open source material includes all necessary information such as key ventilation specifications and the detailed clinical trials data. In order to design a safe and efficient ventilator unit, it is necessary to have a better understanding of the computational modeling of the ventilator system. In reference [3], a fluidic oscillator is proposed to be utilized as educational respiratory simulator unit. In reference [4] a low cost solution based on pneumatic artificial muscles is proposed for mechanical ventilator unit. The proposed solution [4] is cost effective and portable. Safety, reliability and performance of mechanical ventilators are greatly dependent on feedback control techniques. The earlier versions of mechanical ventilators were controlled using classical methods such as proportional, integral (PI) controllers [5]. A pure integral control eliminates steady state error when a step disturbance is applied, however it reduces stability margin of the system. Such controllers with pure integral action are called type-1 controllers. Similarly controllers with one pole-zero pair and additional pole at zero are termed as type-2 controllers. Type-3 controllers consist of three poles and two zeros. Type-1, type-2 and type-3 controllers and its application to mechanical ventilators is reported in reference [6]. However before the advent of microprocessor technology the classical controllers reported above were implemented using analog circuits such as operational amplifiers. In early 90s and with advent of microprocessor technology, classical PID controllers were conveniently implemented for mechanical ventilators [7]. Human lung is modeled as resistance- capacitance (RC) circuit, so during breathing process, dynamics of RC circuit may vary, thus to compensate its effects, an adaptive PI controller is proposed in reference [8]. Similarly a PID controller using optimal control theory is reported in reference [9], and a PID with gain tuning approach is presented in reference [10]. In comparison to classical control methods, modern control methods offer several advantages such as enhanced robustness, easy design of disturbance compensators adaptive loops and ensuring system stability conveniently. However most of the modern control techniques rely on accurate mathematical models of the system. In the existing literature, several model based controllers are reported for mechanical ventilators [11,12]. As mentioned above, the dynamics of human lung may vary during inspiration and expiration process, thus it may deteriorate the closed loop performance if the uncertainties are not properly modeled [13]. Example of some model based controllers that have been specifically applied to mechanical ventilators include model predictive Control [14], variable-gain control [15], and repetitive control [16]. Model predictive controller may suffer from under and over-estimation problem and thus it can compromise patient safety and equipment reliability. Similarly repetitive control has a drawback that it requires accurate knowledge of period time of external signals. Similarly the variable gain controller is applied experimentally, however rigorous stability proof of the closed loop system using modern mathematical theories is lacking. Sliding mode controller (SMC) is widely utilized for systems with known nominal models and known upper bounded disturbances [17,18]. SMC offers high degree of robustness against parameters uncertainty [19,20], However classical SMC controllers introduce high frequency chattering in the excitation signals and it limits the practical applicability of

such controllers [21]. Apart from classical SMC controllers, intelligent controllers such as fuzzy logic control (FLC) and controllers have also been reported and applied to mechanical ventilators [22,23]. In order to ensure optimal control performance of the system with FLC methods [24,25], expert knowledge is required. Moreover it is difficult to adjust and tune fuzzy rules and membership functions [26,27]. A viable solution to minimize chattering in SMC controllers is to combine it with FLC controllers, where a few rules are required to tune discontinuous control gain of SMC controllers [28–31]. Several hybrid controllers based on SMC-FLC method are reported for nonlinear systems [32,33], such as chaotic system, servo mechanism and position servo systems [34–37].

The literature discussed so far is focused on integer order controllers. Recently fractional order (non integer) calculus has found several interesting applications in aerospace systems, biomedical engineering and applied physics. Fractional order systems offer extra degree of freedom to adjust system response optimally. Such controllers have also been applied in the engineering applications such as flight control system [38], renewable energy [39] and biomedical engineering [40]. From the above cited literature it is concluded that fractional order controllers are rarely exploited for biomedical equipment such as mechanical ventilators so in this work we propose to introduce a cascaded robust control scheme for mechanical ventilation using fractional calculus method.

Main contributions of this research work are highlighted as follows:

a) In the existent literature, all previous controller reported for mechanical ventilators are integer order. In this article, non integer control system is also exploited for smooth transition of breathing states.

b) In this article a new methodology is presented based on reduced blower dynamics, which enables the designers to formulate cascaded control system for ventilator unit.

Rest of the paper is organized as follows. In Section 2, the mathematical model of ventilator unit is discussed. In Section 3, controllers are derived, Section 4 discusses the results and finally conclusion is made.

2. Mathematical modeling of ventilator system

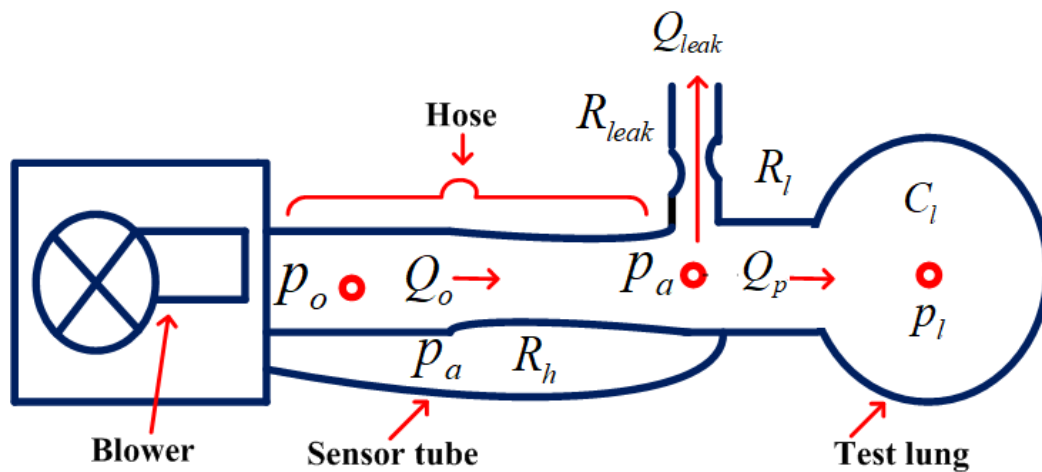
A block diagram of a mechanical ventilator unit is shown in Figure 1 which explains the basic working principle of the respiratory system. In order to develop a detailed mathematical model of a mechanical ventilator, it is necessary to understand the dynamics of its sub components. As shown in Figure 1, a ventilator unit consists of three sub module that include a blower, hose and patient test lungs. The blower unit is actuated by electrical motor and it generates the required pressure for the patient. Hose is utilized to provide a medium between the blower and the patient lungs. Before deriving the detailed mathematical dynamics of the system, the following symbols and parameters are defined in Table 1:

As explained above main job of the blower is to regulate the blowing pressure p_o and linking it to the patient lungs through hose. The patient inhales the air by utilizing the air flow rate Q_o into the lungs with a flow rate of Q_p and exhales the rest of the flow Q_{leak} through hose leak. With the following explanations, the patients, flow dynamics are represented as follows [15]:

$$Q_p = Q_o - Q_{leak} \quad (2.1)$$

Table 1. Nomenclature.

Name	Parameter	Unit
p_o	Desired pressure generated by blower	m-bars
p_a	Airway pressure	m-bars
p_l	Lung pressure	m-bars
p_r	Reference pressure	m-bars
Q_0	Desired flow rate generated by blower	mL/mins
Q_p	Patient flow rate	mL/mins
Q_{leak}	Leak flow rate	mL/mins
R_l	Lung resistance	m-bar/m-L
R_h	Hose resistance	m-bar/m-L
R_{leak}	Leak resistance	m-L/m-bar
C_l	Lungs compliance (Capacitance)	m-bar/m-L

**Figure 1.** Working principle of mechanical ventilator.

By assuming that the nominal resistance of hose, leak channel and patient lungs is known, then the blower, patient and leak flow rates as function of such resistances are expressed as follows:

$$Q_o = \frac{p_o - p_a}{R_h} \quad (2.2)$$

$$Q_{leak} = \frac{p_{leak}}{R_{leak}} \quad (2.3)$$

$$Q_p = \frac{p_a - p_l}{R_l} \quad (2.4)$$

All the parameters of Eqs (2.2)–(2.4) are already defined in Table 1. Lungs pressure dynamics are expressed as follows:

$$\dot{p}_l = \frac{1}{C_l} Q_p \quad (2.5)$$

In Eq (2.5), p_l is analogous to voltage and Q_p is analogous to current. By combining Eqs (2.5) and

(2.6), one obtains the following expression:

$$\dot{p}_l = \frac{p_a - p_l}{R_l C_l} \quad (2.6)$$

By combining Eq (2.1) with Eqs (2.2)–(2.4), the airway pressure p_a is derived in terms of p_o and p_l and the resultant expression is given as follows:

$$p_a = \frac{\frac{1}{R_l} p_l + \frac{1}{R_h p_o}}{\frac{1}{R_h} + \frac{1}{R_l} + \frac{1}{R_{leak}}} \quad (2.7)$$

By combining Eqs (2.6) and (2.7), one obtains the following expression:

$$\dot{p}_l = \frac{-(\frac{1}{R_h} + \frac{1}{R_{leak}}) p_l + \frac{1}{R_h p_o}}{R_l C_l (\frac{1}{R_h} + \frac{1}{R_l} + \frac{1}{R_{leak}})} \quad (2.8)$$

The state space representation of Eq (2.8) is given as follows:

$$\dot{p}_l = a_1 p_l + b_1 p_o \quad (2.9)$$

$$p_a = c_1 p_l + d_1 p_o \quad (2.10)$$

$$Q_p = c_2 p_l + d_2 p_o \quad (2.11)$$

Blower system is modeled as a second order system which is expressed as follows:

$$\dot{x}_{b1} = x_{b2} \quad (2.12)$$

$$\dot{x}_{b2} = a_2 x_{b2} + a_3 x_{b1} + b_2 p_c \quad (2.13)$$

From Eqs (2.12) and (2.13), the states of the blower system are represented as follows: $[x_{b1} \ x_{b2}] = [p_o \ \dot{p}_o]$. Moreover the constants of the state Eqs (2.9)–(2.13) are represented as follows:

$$a_1 = -\frac{\frac{1}{R_h} + \frac{1}{R_{leak}}}{R_l C_l (\frac{1}{R_h} + \frac{1}{R_l} + \frac{1}{R_{leak}})} \quad (2.14)$$

$$b_1 = \frac{\frac{1}{R_h}}{R_l C_l (\frac{1}{R_h} + \frac{1}{R_l} + \frac{1}{R_{leak}})} \quad (2.15)$$

$$c_1 = \frac{\frac{1}{R_l}}{(\frac{1}{R_h} + \frac{1}{R_l} + \frac{1}{R_{leak}})} \quad (2.16)$$

$$c_2 = -\frac{\frac{1}{R_h} + \frac{1}{R_{leak}}}{R_l (\frac{1}{R_h} + \frac{1}{R_l} + \frac{1}{R_{leak}})} \quad (2.17)$$

$$d_1 = \frac{\frac{1}{R_h}}{(\frac{1}{R_h} + \frac{1}{R_l} + \frac{1}{R_{leak}})} \quad (2.18)$$

$$d_2 = \frac{\frac{1}{R_h}}{R_l (\frac{1}{R_h} + \frac{1}{R_l} + \frac{1}{R_{leak}})} \quad (2.19)$$

$$a_2 = -2w_n\zeta \quad (2.20)$$

$$a_3 = -w_n^2 \quad (2.21)$$

In the above equations, w_n represents the natural frequency, ζ is the damping ratio and p_c represents the control excitation signal of the blower motor. In practice the matrices/parameters defined above may vary over time due to the inclusion of resistance and capacitance terms of the lung, blower and hose so the resultant state space model with introduced parametric uncertainty is expressed as follows:

$$\begin{bmatrix} \dot{p}_l = a_1 p_l + b_1 p_o + D_{p_l} \\ p_a = c_1 p_l + d_1 p_o + D_{p_a} \\ Q_p = c_2 p_l + d_2 p_o + D_{Q_p} \end{bmatrix} \quad (2.22)$$

$$\begin{bmatrix} \dot{x}_{b1} = x_{b2} \\ \dot{x}_{b2} = a_2 x_{b2} + a_3 x_{b1} + b_2 p_c \end{bmatrix} \quad (2.23)$$

In Eq (2.22), the disturbance terms are defined as follows:

$$D_{p_l} = \Delta a_1 p_l + \Delta b_1 p_o \quad (2.24)$$

$$D_{p_a} = \Delta c_1 p_l + \Delta d_1 p_o \quad (2.25)$$

$$D_{Q_p} = \Delta c_2 p_l + \Delta d_2 p_o \quad (2.26)$$

here Δa_1 , Δb_1 , Δc_1 , Δd_1 , Δc_2 and Δd_2 represent the uncertainty in the system matrices.

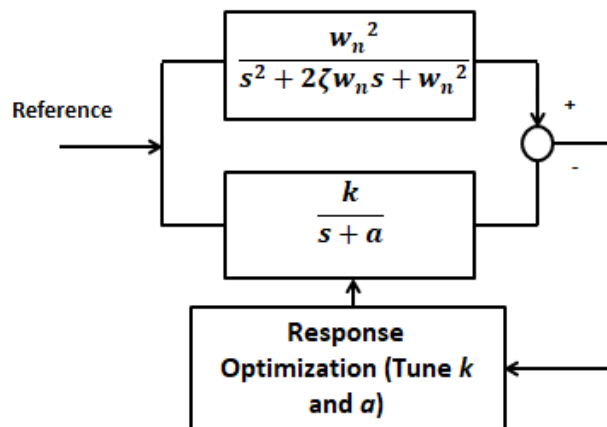


Figure 2. Blower model approximation using response optimization tool box.

In order to design the cascaded controller, the second order dynamics of the blower presented in Eq (2.23) are approximated using first order system. The approximation is done using MATLAB response optimization toolbox and the first order system is tuned until the response of both 2nd order blower model and the 1st order approximated system closely coincides. The parameters of blower model given in [15] are utilized to approximate the 1st order model. The utilized parameters for blower unit are as follows [15]: $w_n = 2\pi 30$ and $\zeta = 1$. With these parameters, the transfer function of the blower system

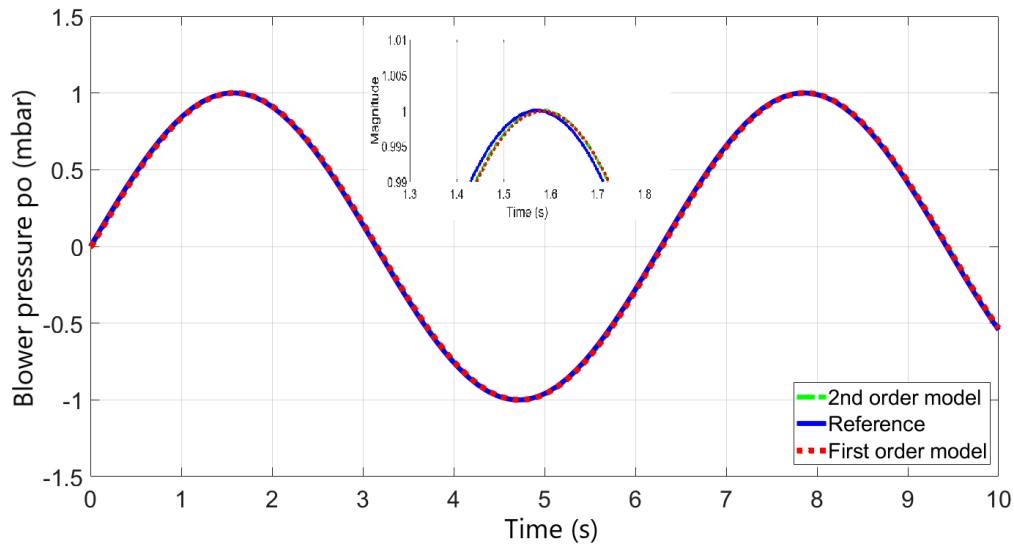


Figure 3. Blower model fitting response for sinusoidal reference.

is represented as follows:

$$\frac{p_o}{p_c} = \frac{(2\pi 30)^2}{s^2 + 4\pi 30s + (2\pi 30)} \quad (2.27)$$

A generalized first order blower system model with one pole is expressed as follows:

$$\frac{p_o}{p_c} = \frac{k}{s + a} \quad (2.28)$$

In Eq (2.28), k and a are estimated using response optimization toolbox such that the error between the output of Eqs (2.27) and (2.28) is very small. Figure 2 explains the model approximation process of the blower unit. The estimated parameters are recorded as follows: $k = 80$ and $a = 80$. Figures 3 and 4 show the comparison of the output responses of the 2nd order and approximated first order models with step and sinusoidal references. From the presented results it is concluded that the approximated first order model represents the blower 2nd order dynamics closely. From Eq (2.28) and by using the identified parameters, the simplified first order model of the blower system is expressed in state space which is given as follows:

$$\dot{p}_o = -ap_o + kp_c \quad (2.29)$$

3. Cascaded control system formulation

Main objective of the closed loop control system is to regulate the airway pressure p_a , ensure smooth supply of patient air flow Q_p and smooth transition of patient airflow Q_p between various levels. In order to ensure patient safety, a lot of care is to be taken in choosing the appropriate control law. As explained in the abstract, an ideal control system shall ensure quick and smooth air pressure buildup and release with minimum overshoots and oscillations in the control excitation signals. So based on the above discussions, a robust controller based on integer calculus is derived as a first step, and then the method

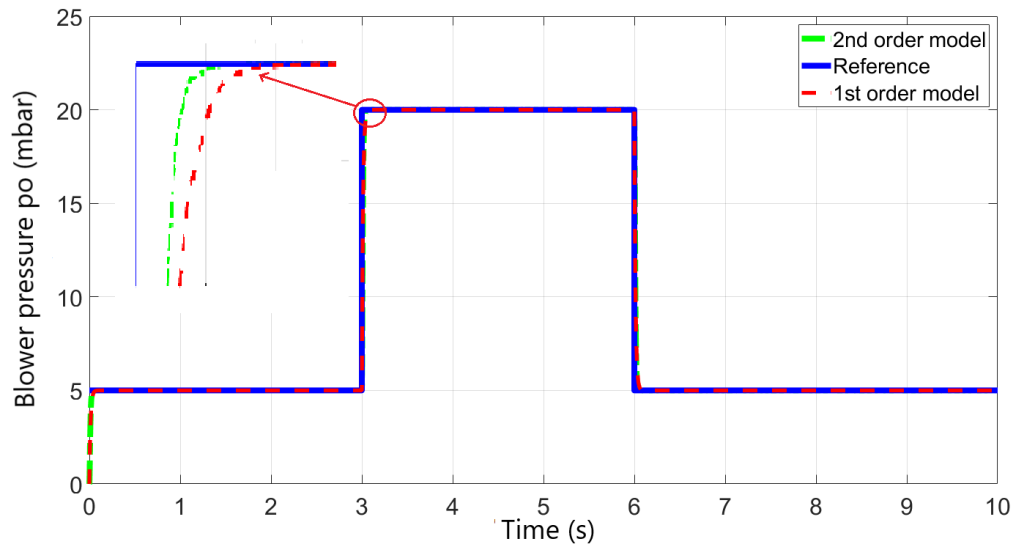


Figure 4. Blower model fitting response for step reference.

is generalized to non integer control method. The motivation behind the introduction of non integer robust control system is to smoothly regulate the patient pressure and flow, the details of which are presented in Figure 5.

Steps in the derivation of cascaded control:

- 1) From Eq (2.22), take the first derivative of airway pressure p_a and represent the resultant dynamics as \dot{p}_a .
- 2) From Eq (2.22), combine the dynamics of lung pressure \dot{p}_l into \dot{p}_a .
- 3) From the resultant \dot{p}_a , derive the control law as \dot{p}_0 .
- 4) The derived airway pressure control law \dot{p}_0 is equated to the approximated blower dynamics of Eq (2.28) to formulate the blower control law p_c .

Note: The above steps enable the designers to cascade the blower dynamics in the airway pressure control law.

Keeping in view the breathing cycle presented in Figure 5, the closed loop controller should ensure the following performance indices:

- 1: The transition between inspiration and expiration cycle should be smooth and oscillations free.
- 1: Patient flow should be oscillations and overshoots free.

The following assumptions are made for deriving the proposed controllers.

Assumption 1: Patient lung pressure is approximated using $p_l = p_a - Q_p R_l$. it is assumed that the patient flow rate Q_p is measurable.

Assumption 2: The parametric uncertainty is upper bounded such that the following relations hold true: $\Delta a_1 \leq \sigma_1$, $\Delta b_1 \leq \sigma_2$, $\Delta c_1 \leq \sigma_3$, $\Delta c_2 \leq \sigma_4$, $\Delta d_1 \leq \sigma_5$, $\Delta d_2 \leq \sigma_6$. Here $\sigma_1 \rightarrow \sigma_6$ represent positive known constants. Before deriving the controllers, basic explanations of fractional calculus are presented below.

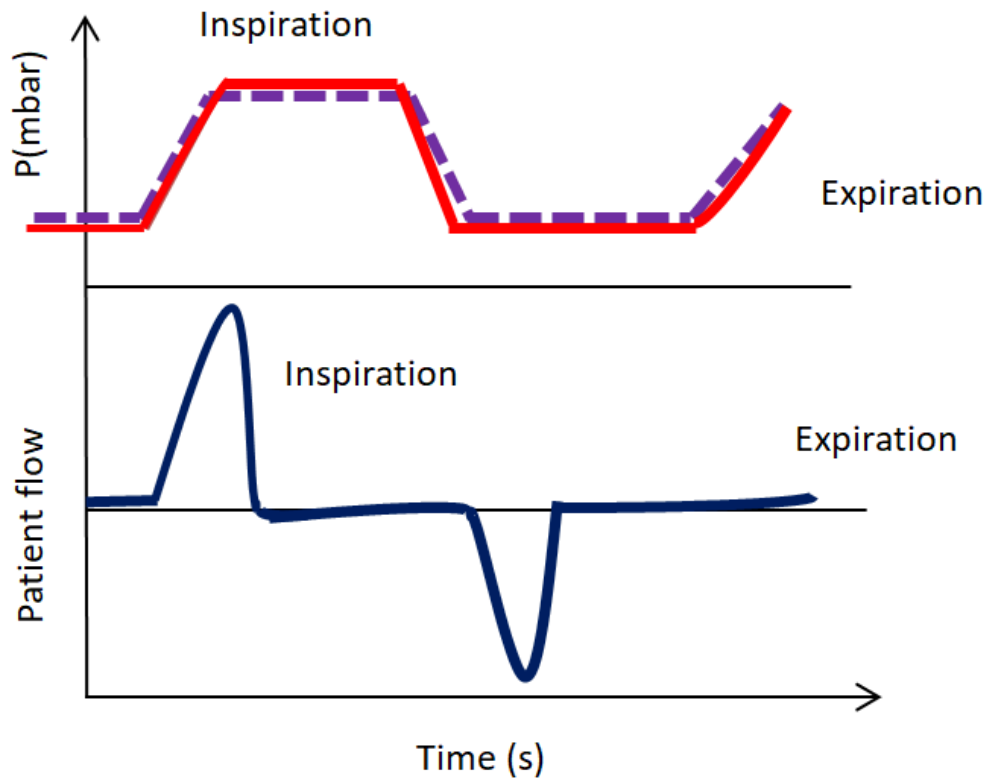


Figure 5. Patient breathing cycle with mechanical ventilation.

3.1. Basics of non integer calculus

The fundamental fractional operator ${}_aO_t^\alpha$ is represented as follows: [38].

$${}_aO_t^\alpha \cong O^\alpha = \begin{cases} \frac{d^\alpha}{dt^\alpha} & R(\alpha) > 0 \\ 1 & R(\alpha) = 0 \\ \int_a^t (d\tau) & R(\alpha) < 0 \end{cases} \quad (3.1)$$

A fractional operator is approximated by three different methods discussed below [39]:

Definition 1. Riemann–Liouville Operator :

$${}_aO_t^{-\alpha} f(t) = \frac{d^\alpha}{dt^\alpha} f(t) = \frac{1}{\Gamma(z-\alpha)} \int_a^t \frac{f(\tau)}{(t-\tau)^{\alpha-z+1}} d\tau \quad (3.2)$$

$${}_aO_t^{-\alpha} f(t) = I^\alpha f(t) = \frac{1}{\Gamma(\alpha)} \int_a^t \frac{f(\tau)}{(t-\tau)^{1-\alpha}} d\tau \quad (3.3)$$

where z is an integer which satisfies the following: $z \geq \alpha$, $(z-1) < \alpha < z$ and $(t-\alpha)$ represents limits of integration. Γ represents the Euler's function.

Definition 2. α^{th} order Non integer derivative of a function using Caputo definition is expressed in Eq (3.4) [38]:

$${}_aO_t^\alpha \cong O^\alpha = \begin{cases} \frac{1}{\Gamma(n-\alpha)} \int_a^t \frac{f^n(\tau)}{(t-\tau)^{\alpha-n+1}} d\tau & n-1 \leq \alpha < n \\ \frac{d^n}{dt^n} f(t) & \alpha = n \end{cases} \quad (3.4)$$

Definition 3. Grunwald–Letnikov definition is expressed as follows [38]:

$${}_aO_t^\alpha(f(t)) = \lim_{h \rightarrow 0} \frac{1}{h^\alpha} \sum_{j=0}^{[(t-\alpha)/h]} (-1)^j \binom{\alpha}{j} f(t-jh) \quad (3.5)$$

In Eq (3.5), h represents the time step.

$$\binom{\alpha}{j} = \frac{\Gamma(\alpha+1)}{\Gamma(j+1)\Gamma(\alpha-j+1)} \quad (3.6)$$

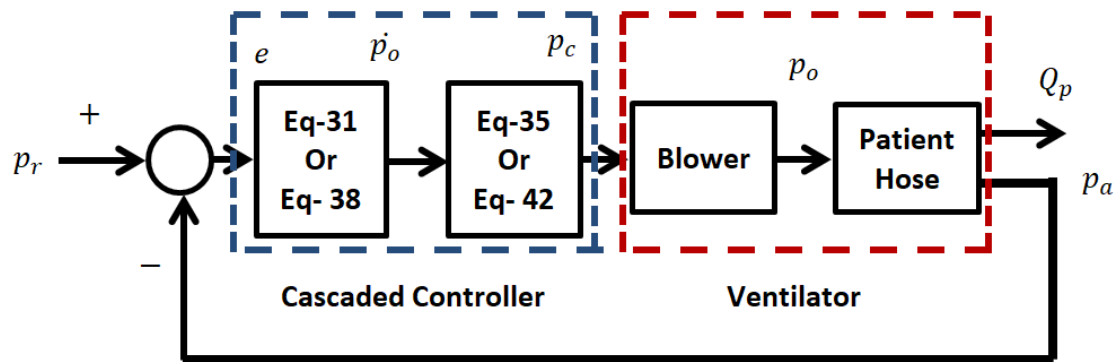


Figure 6. Block diagram of cascaded controllers.

3.2. Integer order control based on linear sliding surface

In this sub-section cascaded integer order sliding mode controller is formulated for airway pressure regulation problem of mechanical ventilator. Let the reference pressure command is denoted by p_r , then the airway pressure error is expressed as follows: $e = p_r - p_a$. By taking the first derivative of the the error term and combining it with the sliding surface S yields the following detailed expression:

$$S_{integer} = g_1(p_r - p_a) + g_2 \int e \quad (3.7)$$

From Eq (2.22), by taking the first time derivative of the airway pressure p_a and combining it with the dynamics of lung pressure yields the following expression:

$$\dot{p}_a = c_1 a_1 p_l + c_1 b_1 p_o + c_1 D_{p_l} + d_1 \dot{p}_o + \dot{D}_{p_a} \quad (3.8)$$

By combining the first derivative of Eq (3.7) with Eq (3.8) one obtains the following expression:

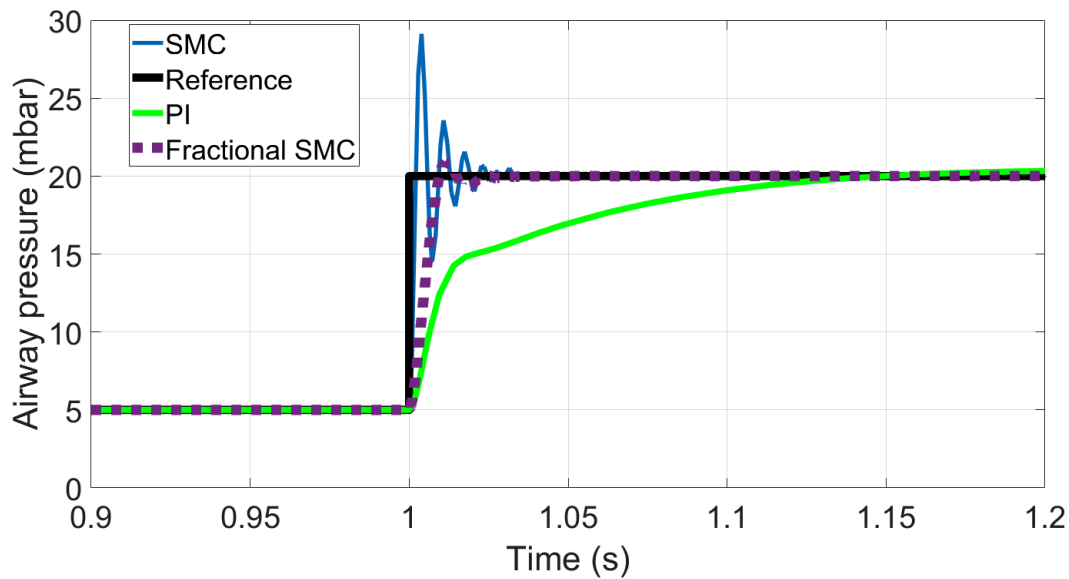


Figure 7. Enlarged view1 of airway pressure tacking.

$$\dot{S}_{integer} = g_1(\dot{p}_r - c_1 a_1 p_l - c_1 b_1 p_o - c_1 D_{pl} - d_1 \dot{p}_o - \dot{D}_{pa}) + g_2 e \quad (3.9)$$

From Eq (3.9), the first derivative of airway pressure control action is expressed as follows:

$$\dot{p}_o = \frac{1}{d_1}(\dot{p}_r - c_1 a_1 p_l - c_1 b_1 p_o + \frac{g_2}{g_1} e + \frac{\eta_1}{g_1} \text{sgn}(S_{integer})) \quad (3.10)$$

Theorem 1. *The control paradigm of Eq (3.10) stabilizes the system dynamics of Eq (2.22) and forces the airway pressure error e in the vicinity of the equilibrium point.*

Proof. In order to prove system stability, the Lyapunov function is defined as follows:

$$V_{integer} = \frac{1}{2} S_{integer}^2 \quad (3.11)$$

The following points are true for the Lyapunov function of Eq (3.11).

- 1) $V_{integer} \rightarrow 0$ when $S_{integer} \rightarrow 0$.
- 2) $V_{integer} \rightarrow \infty$ when $S_{integer} \rightarrow \infty$.

For the closed loop system stability the first time derivative of the Lyapunov function must be less than or equal to zero i.e., $\dot{V}_{integer} \leq 0$. By combining Eq (3.9) and Eq (3.10) with the first time derivative of Eq (3.11), one obtains the following simplified relation:

$$\dot{V}_{integer} = -\eta_1 |S_{integer}| - (c_1 S_{integer} D_{pl} + S_{integer} \dot{D}_{pa}) \quad (3.12)$$

In Eq (3.12), $\dot{V}_{integer} \leq 0$ if $\eta_1 \geq c_1 D_{pl-max} + \dot{D}_{pa-max}$. Here D_{pl-max} and \dot{D}_{pa-max} represent the upper limits of the mentioned disturbance terms. From Eq (3.12), we have the following cases:

- 1) When $S_{integer}$ is negative; D_{pl} is negative; \dot{D}_{pa} is negative so the sum term $(c_1 S_{integer} D_{pl} + S_{integer} \dot{D}_{pa})$ is also negative, and with $\eta_1 |S_{integer}| \geq c_1 (\text{sum terms})$, $\dot{V}_{integer} \leq 0$.

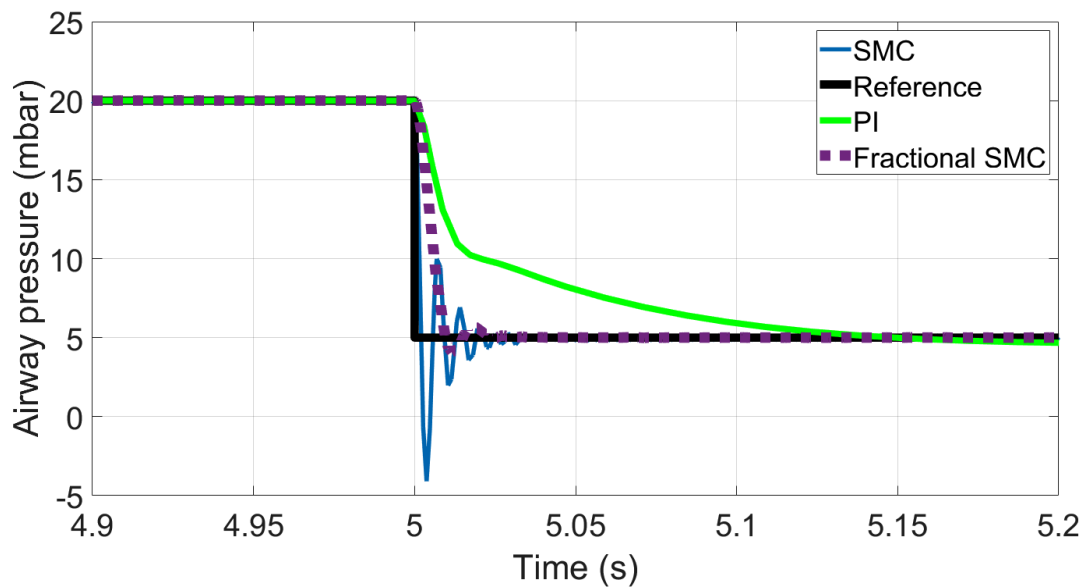


Figure 8. Enlarged view-2 of airway pressure tacking

2) When $S_{integer}$ is positive; D_{pl} is negative; \dot{D}_{pa} is negative so the sum term $(c_1 S_{integer} D_{pl} + S_{integer} \dot{D}_{pa})$ is positive, and with $\eta_i |S_{integer}| \geq c_1 (\text{sum terms})$, $\dot{V}_{integer} \leq 0$. Now the blower control law p_c is cascaded with the airway pressure control law by combining Eqs (2.29) and (3.10) which is obtained as follows:

$$\frac{1}{d_1}(\dot{p}_r - c_1 a_1 p_l - c_1 b_1 p_o + \frac{g_2}{g_1} e + \frac{\eta_1}{g_1} \text{sgn}(S_{integer})) = -a p_o + k p_c \quad (3.13)$$

Equation (3.13) is simplified and expressed in terms of blower control law as follows:

$$p_c = k^{-1} [\frac{1}{d_1}(\dot{p}_r - c_1 a_1 p_l - c_1 b_1 p_o + \frac{g_2}{g_1} e + \frac{\eta_1}{g_1} \text{sgn}(S_{integer})) + a p_o] \quad (3.14)$$

Equation (3.14) represents the blower controller p_c cascaded with the dynamics of the airway pressure. \square

3.3. Fractional order control

In this section a fractional order cascaded controller is derived for airway pressure regulation problem. With the defined airway pressure e , a fractional order sliding surface $S_{fractional}$ is defined as follows:

$$S_{fractional} = g_1 D^\alpha (p_r - p_a) + g_2 \int e \quad (3.15)$$

where D^α represents fractional derivative with order α . By combining the first derivative of Eq (3.15) with Eq (3.8), one obtains the following expression:

$$\dot{S}_{fractional} = g_1 D^\alpha (\dot{p}_r - c_1 a_1 p_l - c_1 b_1 p_o - c_1 D_{pl} - d_1 \dot{p}_o - \dot{D}_{pa}) + g_2 e \quad (3.16)$$

From Eq (3.16), the first derivative of airway pressure control action is expressed as follows:

$$\dot{p}_o = \frac{1}{d_1} (\dot{p}_r - c_1 a_1 p_l - c_1 b_1 p_o + \frac{g_2}{g_1} D^{-\alpha} e + \frac{\eta_1}{g_1} D^{-\alpha} \text{sgn}(S_{fractional})) \quad (3.17)$$

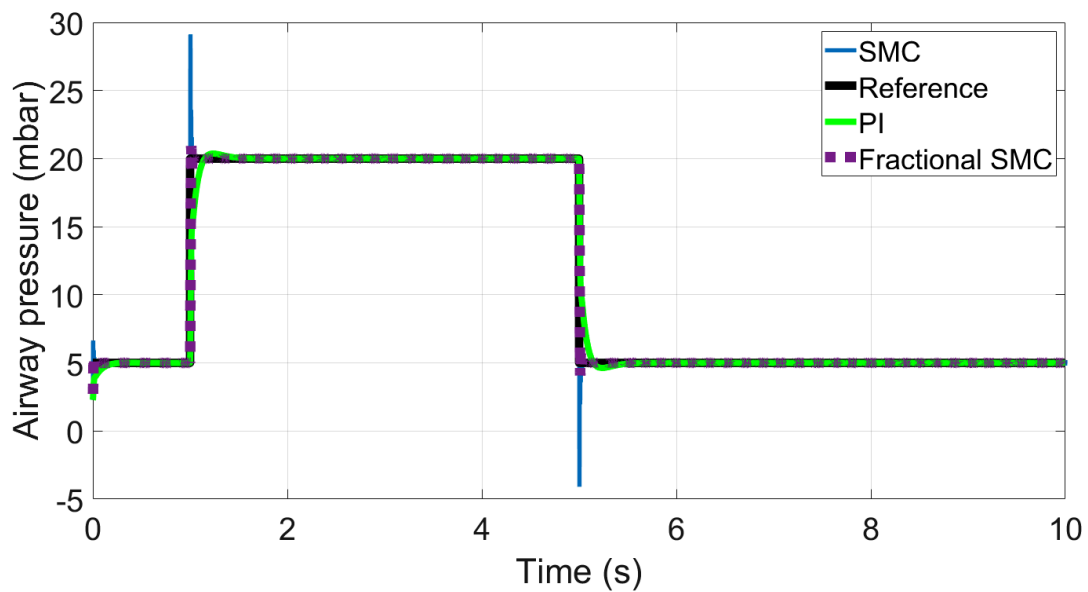


Figure 9. Airway pressure tracking response comparison.

The derived controller consists of fractional integrator taken around the error term and signum function. Thus the dynamics of the derived controller Eq (3.17) are different from the one we derived in Eq (3.1).

Theorem 2. *The control paradigm of Eq (3.17) stabilizes the system dynamics of Eq (2.22) and forces the airway pressure error e in the vicinity of the equilibrium point.*

Proof. In order to prove system stability, the Lyapunov function is defined as follows:

$$V_{fractional} = \frac{1}{2} S_{fractional}^2 \quad (3.18)$$

The following points are also true for the Lyapunov function of Eq (3.18).

1. $V_{fractional} \rightarrow 0$ when $S_{fractional} \rightarrow 0$.
2. $V_{fractional} \rightarrow \infty$ when $S_{fractional} \rightarrow \infty$.

For the closed loop system stability the first time derivative of the Lyapunov function must be less than or equal to zero i.e., $\dot{V}_{fractional} \leq 0$. By combining Eqs (3.16), (3.17) with the first derivative of Eq (3.18), one obtains the following relation:

$$\dot{V}_{fractional} = -\eta_1 |S_{fractional}| - (c_1 S_{fractional} \dot{D}_{pl} + S_{fractional} \dot{D}_{pa}) \quad (3.19)$$

In Eq (3.19), $\dot{V}_{fractional} \leq 0$ by choosing $\eta_1 \geq c_1 \dot{D}_{pl-max} + \dot{D}_{pa-max}$.

Now a fractional order blower control law p_c is derived by combining Eqs (2.29) and (3.17) and expressed as follows:

$$\frac{1}{d_1} (\dot{p}_r - c_1 a_1 p_l - c_1 b_1 p_o + \frac{g_2}{g_1} D^{-\alpha} e + \frac{\eta_1}{g_1} D^{-\alpha} \text{sgn}(S_{fractional})) = -a p_o + k p_c \quad (3.20)$$

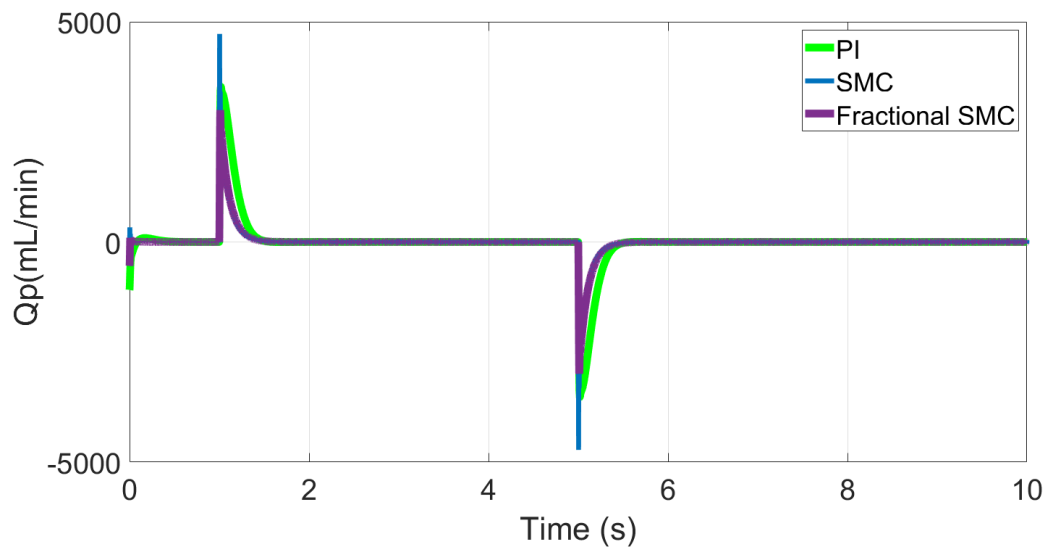


Figure 10. Patient flow rate response comparison.

Equation (3.20) is simplified and expressed in terms of blower control law as follows:

$$p_c = k^{-1} \left[\frac{1}{d_1} (\dot{p}_r - c_1 a_1 p_l - c_1 b_1 p_o + \frac{g_2}{g_1} D^{-\alpha} e + \frac{\eta_1}{g_1} D^{-\alpha} \text{sgn}(S_{\text{fractional}})) + a p_o \right] \quad (3.21)$$

A block diagram of the cascaded control scheme is shown in Figure 6.

Note: Comparing the control laws presented in Eqs (3.14) and (3.21), the fractional order control law offers additional degree of freedom in the discontinuous part i.e., $D^{-\alpha} \text{sgn}(S_{\text{fractional}})$, where adjusting the order of fractional integrator $D^{-\alpha}$ will lead to smooth out the oscillations of the $\text{sgn}(\cdot)$ term and also it will allow a fair degree of robustness to uncertainties. In comparison to non-integer controller, the discontinuous part of integer controller Eq (3.14) will excite high frequency oscillations and thus it cannot be utilized in practice.

□

4. Results and discussion

In this section the system is simulated with the integer and non integer controllers discussed in the previous section. In order to show the limitations of classical controllers, the ventilator system is also tested using PI controller and the obtained results are compared with the proposed controllers. The parameters of the ventilator unit are tabulated in Table 2 [15]. The parameters of the controllers are tuned using MATLAB response optimization toolbox for the given reference signal of p_r . The tuned parameters of the controllers are shown in Table 3.

The ventilator is tested under the following two conditions. 1) With constant system parameters (ideal condition testing). 2) With parameters uncertainty (Robustness test).

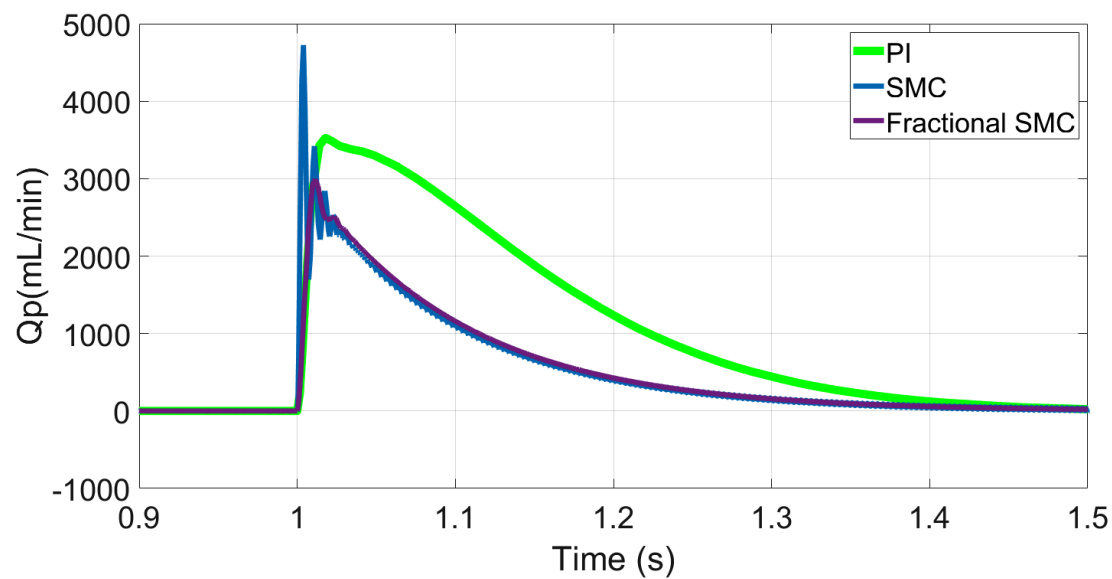


Figure 11. Enlarged view1 of patient flow rate response.

Table 2. Ventilator System Parameters.

Parameter	Value	Unit
R_l	5/1000	mbar/mL
C_l	20	mL/mbar
R_{leak}	60/1000	mbar/mL
R_h	4.5/1000	mbar/mL
w_n	$2\pi \ 30$	rad/s

Table 3. Control System Parameters.

SMC	Value	Fractional SMC	Value	PI	Value
g_1	3	g_1	3	k_p	3
g_2	500	g_2	500	k_i	250
η_1	150	η_1	150	—	—
—	—	α	0.65	—	—

4.1. Test under ideal conditions

In the first test, the parameters of the ventilator unit are treated as constant. System parameters a_1 , b_1 , c_1 , c_2 , d_1 and d_2 are calculated from the another set of parameters tabulated in Table 2. The

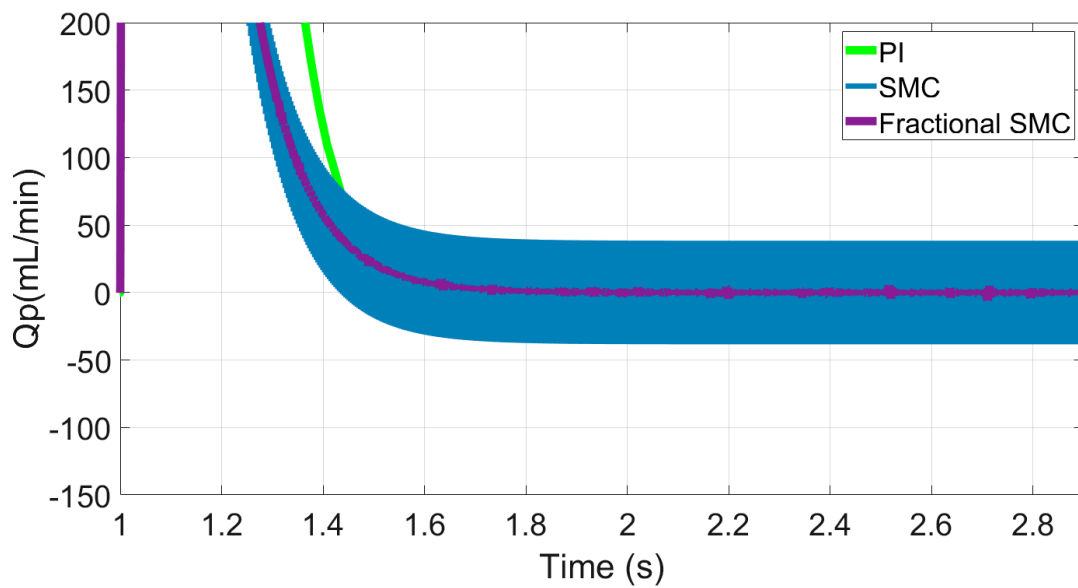


Figure 12. Enlarged view2 of patient flow rate response.

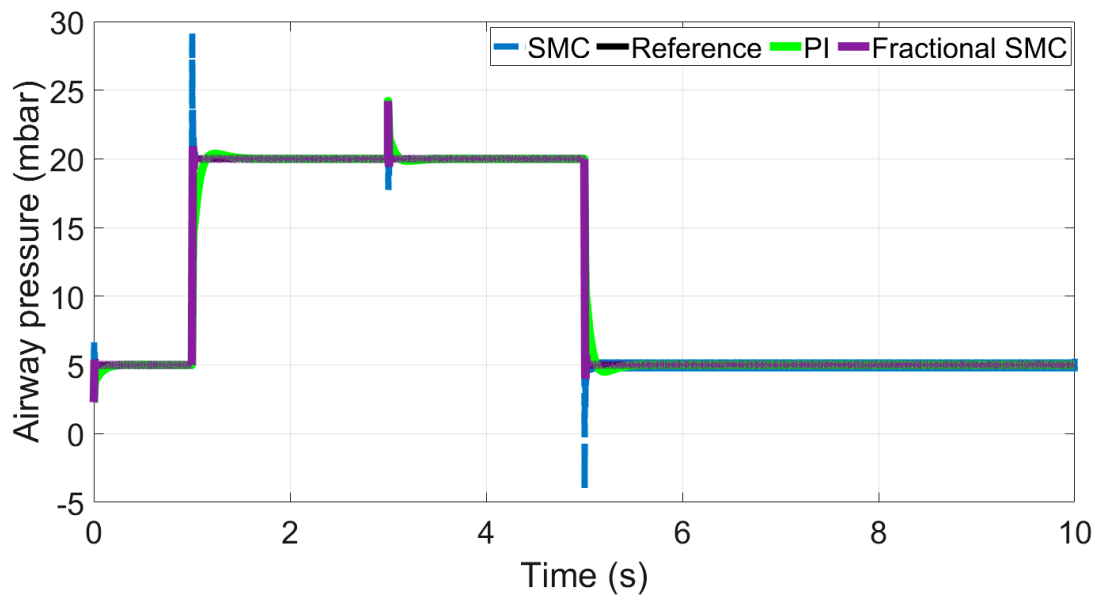


Figure 13. Airway pressure tracking comparison.

reference airway pressure command p_r is chosen as follows:

$$p_r = \begin{cases} 5 \text{ mbar} & t = (0 \rightarrow 1)s \\ 20 \text{ mbar} & t = (1 \rightarrow 5)s \\ 5 \text{ mbar} & t = (5 \rightarrow 10)s \end{cases} \quad (4.1)$$

Figure 7 shows the tracking response of airway pressure with integer order SMC, fractional order SMC and PI controllers respectively. Since there are two abrupt changes in reference command at

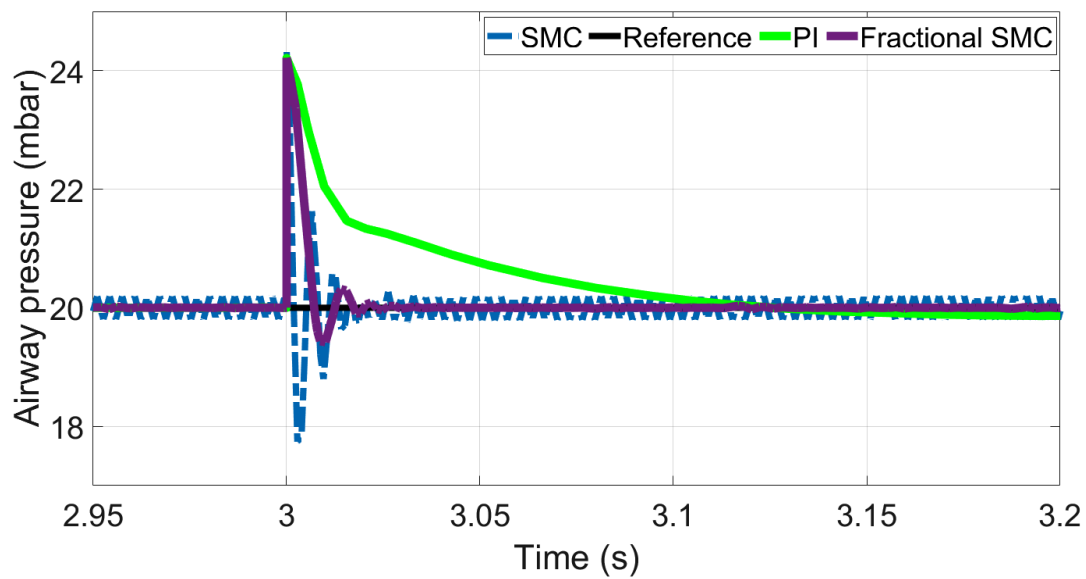


Figure 14. Enlarge tracking view of airway pressure.

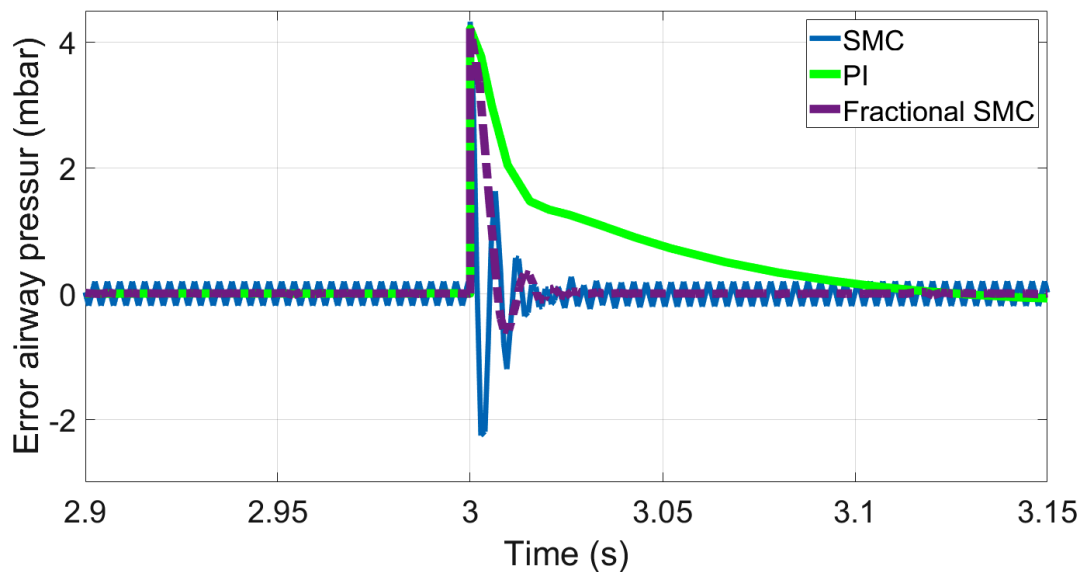


Figure 15. Airway pressure error tracking response comparison.

$t = 1$ s and 5 s so in order to have a better visibility of the presented results, two enlarged views of Figure 7 at time $t = 1$ s and 5 s are shown in Figures 8 and 9. As shown in Figures 8 and 9, airway pressure tracking offers high oscillations with SMC controller at $t = 1$ s and 5 s. Overshoots reaching peak values of 29 mbar and -4.9 mbar are recorded at $t = 1$ s with classical SMC controller. Moreover with integer order SMC controller, the oscillations are settled out at 1.04 s and 5.04 s respectively. The reason is very obvious as because the sliding surface presented in Eq (3.7) is a PI type so the integral gain g_2 improves the rise time but at the cost of transient oscillations. Such responses exhibited by classical SMC controllers are not good because it sets oscillatory air flow for patient lungs in the event

of any transient. Similarly for PI controller, the integral gain k_i is chosen such that it is less than g_2 gain of the SMC. With a lower integral gain as compared to the SMC, the tracking response of the ventilator unit is poor with slow rise time. here it is worth to mention that with increase of integral gain for PI controller, system would again excite unwanted overshoots and oscillations as these were observed in the case of SMC controller. In comparison to the SMC and PI controllers, the proposed fractional order SMC controller offers superior performance in terms of rise time, low oscillations and improved settling time. Overshoots reaching peak values of 21 mbar and 4.9 mbar are recorded at $t = 1$ s with fractional order SMC controller. Moreover with fractional order SMC controller, the oscillations are settled out abruptly. The response comparison of patient flow rate Q_p with the discussed controllers are given in Figures 10–12. Figure 10 shows that with SMC controller, high overshoot of flow rates are experienced by patient at time $t = 1$ s and 5 s, while with PI controller, the flow rate response is delayed. Figures 11 and 12 present a better view of the patient flow rate with fractional order SMC controller. From the presented results, an overshoot of 4800 mL/min is observed in the patient flow Q_p with integer order SMC controller at time $t = 1$ s while the peak recorded value of Q_p with fractional order SMC controller is 3000 mL/min. Although PI also offers the same peak overshoot as of fractional order SMC controller, however PI controller exhibits a delayed response. Integer order SMC offers high frequency chattering in the airflow Q_p and with such high frequency oscillations, safety of the patient may compromise. The proposed fractional order SMC offers smooth patient air flow with improved rise time and less oscillations.

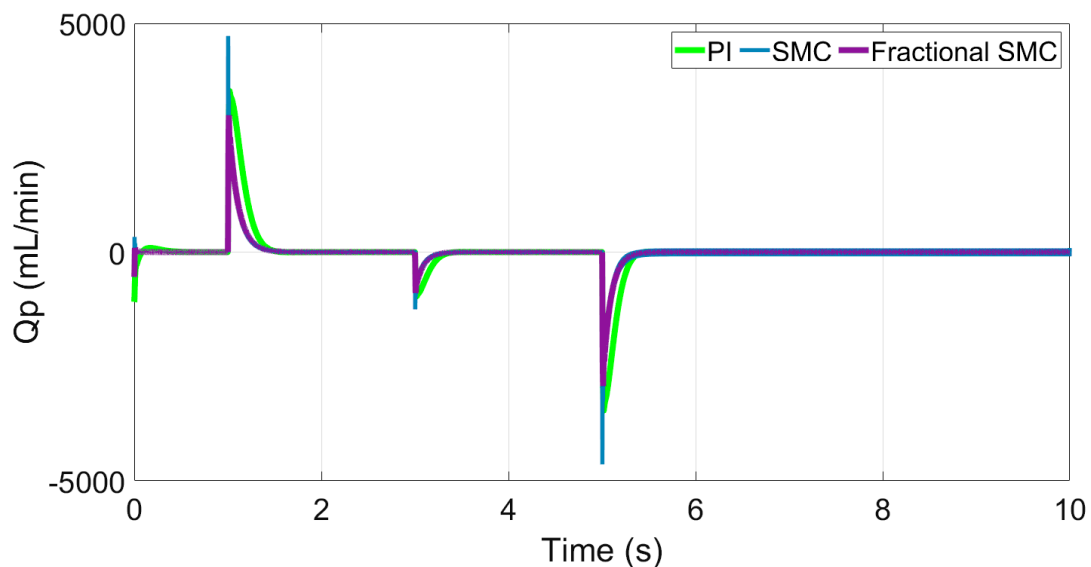


Figure 16. Patient flow rate response comparison.

4.2. Robustness test

In the second test, the parameters of the ventilator unit are subject to the following uncertainty: $D_{p_l} = -0.01a_1p_l + 0.01b_15p_o$ and $D_{p_a} = -0.25c_1p_l + 0.01d_1p_o$. Reference airway pressure p_r is the same as given in Eq (4.1). The disturbance terms are applied at $t = 3$ s. With these conditions, the tracking response comparison of airway pressure with SMC, fractional order SMC and PI controllers

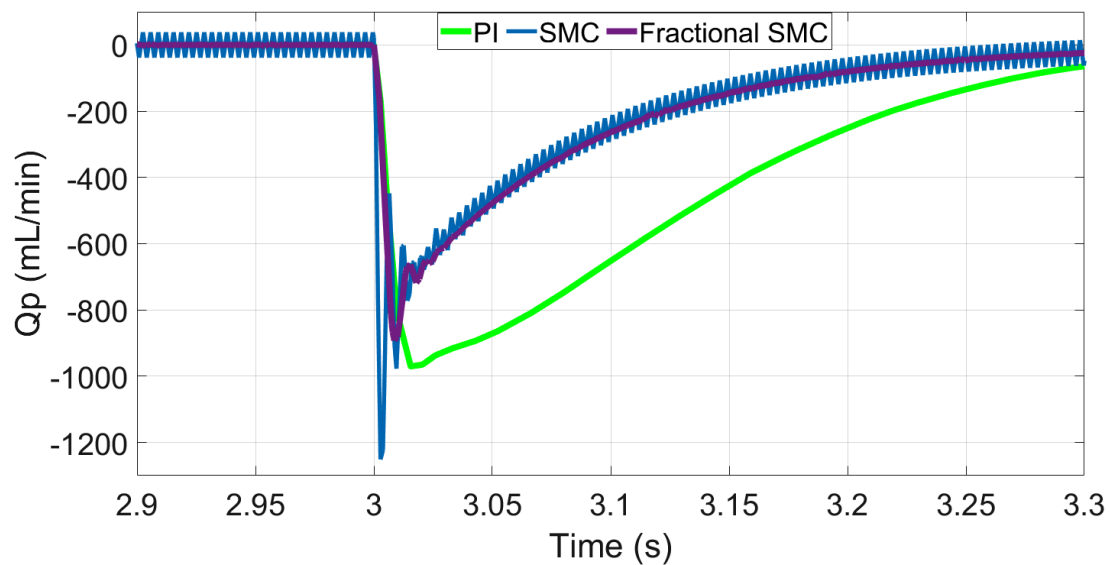


Figure 17. Enlarged view of patient flow rate response comparison.

is shown in Figure 13. In order to have better visibility of the results, the enlarge view of the airway pressure at time $t = 3$ s and its error response are plotted in Figures 14 and 15. From the presented results of Figures 14 and 15, it is notable that at time $t = 3$ s, a peak overshoot of 4 mbar is recorded with SMC, fractional SMC and PI controllers respectively. However SMC suffers from oscillations of large magnitude while PI controller introduces a lagging response. Fractional order SMC controller offers a comparable response of the rise and settling times as of SMC with additional advantage of suppressing the high frequency oscillations in the control signal. Similarly the patient flow rate is simulated and compared in Figures 16 and 17. Figure 17 shows enlarged view of patient flow Q_p where only the time interval of uncertainty application is under considerations i.e., $t = 3$ s. The uncertainty terms are applied at time $t = 3$ s and from the presented results, a peak overshoot of -1200 mL/min is recorded with SMC controller while with the proposed controller the recorded overshoot is approximately -1000 mL/min. PI controller also exhibits a peak of -1000 mL/min in the patient flow Q_p , however it adds a delay in the response. It is obvious from the results presented in Figure 17, that the proposed fractional order SMC controller offers smooth airflow to the patient without high frequency oscillations, while integer order SMC controller offers high frequency oscillations.

5. Conclusions

In this article we presented a novel method to derive cascaded robust control system for a ventilator unit using blower model reduction techniques. The blower dynamics are compensated in the final control law. In order to verify that the mechanical ventilator unit meets the defined ideal characteristics with the proposed control law, two tests namely 1. test under ideal conditions 2. robustness test are performed. From the presented results, airway pressure tracking offers high oscillations with integer order SMC controller at $t = 1$ s and 5 s. Overshoots peak values of 29 mbar and -4.9 mbar are recorded at $t = 1$ s with classical SMC controller. Moreover with integer order SMC controller, the

oscillations are settled out at 1.04 s and 5.04 s respectively. In comparison to integer order SMC controller, the proposed fractional order SMC controller offers superior performance in terms of rise time, low oscillations and improved settling time in the airway pressure. Overshoots peak values of 21 mbar and 4.9 mbar are recorded at $t = 1$ s with fractional order SMC controller. Moreover with fractional order SMC controller, the oscillations are settled out abruptly. The proposed fractional order controller offers advantages such as robustness, fast rise and minimum settling time response in comparison to the integer order SMC method. Utilization of high computational resources is a major disadvantage of the proposed fractional control system. This particular issue can be addressed by utilizing the concepts presented in reference [41].

6. Future work

In general fractional order controllers utilize high computational resources as compared to integer order methods. A novel idea for minimization of computational resources for non-integer controllers is reported in [41]. An interesting future application of the ideas presented in [41] is to extend the same for mechanical ventilators. Another future aspect is to conduct experiments with test lungs and qualify the performance indices of the proposed controller.

Acknowledgments

This work was supported by Taif University Researchers Supporting Project number (TURSP-2020/144), Taif University, Taif, Saudi Arabia

Conflict of interest

The authors declare there is no conflict of interest.

References

1. C. Wu, X. Chen, Y. Cai, J. Xia, X. Zhou, S. Xu, et al., Risk factors associated with acute respiratory distress syndrome and death in patients with coronavirus disease 2019 pneumonia in Wuhan, China, *JAMA Intern. Med.*, **180** (2020), 934–943. doi:10.1001/jamainternmed.2020.0994.
2. MIT, *MIT emergency ventilator project*, 2021. Available from: <https://emergency-vent.mit.edu>.
3. T. Dillon, C. Ozturk, K. Mendez, L. Rosalia, S. D. Gollob, K. Kempf, et al., Computational modeling of a low-cost fluidic oscillator for use in an educational respiratory simulator, *Adv. NanoBiomed Res.*, **2021** (2021), 2000112. doi: 10.1002/anbr.202000112.
4. S. M. Mirvakili, D. Sim, R. Langer, Inverse pneumatic artificial muscles for application in low-cost ventilators, *Adv. Intell. Syst.*, **3** (2021), 1–11. doi: 10.1002/aisy.202000200.
5. M. Borrello, Modeling and control of systems for critical care ventilation, in *IEEE Proceedings of the 2005, American Control Conference*, **3** (2005), 2166–2180. doi: 10.1109/ACC.2005.1470291.
6. M. Walter, S. Leonhardt, Control applications in artificial ventilation, *IEEE Mediterr. Conf. Control Automation*, **2007** (2007), 1–6. doi: 10.1109/MED.2007.4433762.

7. K. B. Ohlson, D. R. Westenskow, W. S. Jordan, A microprocessor based feedback controller for mechanical ventilation, *Ann. Biomed. Eng.*, **10** (1982), 35–48. doi: 10.1007/BF02584213.
8. M. Borrello, Adaptive control of a proportional flow valve for critical care ventilators, in *ACC Annual American Control Conference*, (2018), 104–109. doi: 10.23919/ACC.2018.8431425.
9. Y. Xu, L. Li, J. Yan, Y. Luo, An optimized controller for bi-level positive airway pressure ventilator, in *International Conference on Future Computer and Communication Engineering*, **149** (2014), 149–152. doi: 10.2991/icfcce-14.2014.37.
10. D. Acharya, D. K. Das, Swarm optimization approach to design PID controller for artificially ventilated human respiratory system, *Comput. Methods Programs Biomed.*, **198** (2021), 105776. doi: 10.1016/j.cmpb.2020.105776.
11. E. Martinoni, C. A. Pfister, K. Stadler, P. Schumacher, D. Leibundgut, T. Bouillon, et al., Model-based control of mechanical ventilation: design and clinical validation, *Br. J. Anaesth.*, **92** (2004), 800–807. doi: 10.1093/bja/aeh145.
12. M. Scheel, T. Schauer, A. Berndt, O. Simanski, Model-based control approach for a cpap-device considering patient's breathing effort, *IFAC Papers OnLine*, **50** (2017), 9948–9953. doi: 10.1016/j.ifacol.2017.08.1572.
13. S. Korrapati, J. S. Yang, Adaptive inverse dynamics control for a two compartment respiratory system, in *IEEE International Conference on Consumer Electronics-Taiwan*, (2016), 1–2. doi: 10.1109/ICCE-TW.2016.7521037.
14. H. Li, W. M. Haddad, Model predictive control for a multi compartment respiratory system, *IEEE Trans. Control Syst. Technol.*, **21** (2012), 1988–1995. doi: 10.1109/TCST.2012.2210956.
15. B. Hunnekens, S. Kamps, N. Van De Wouw, Variable-gain control for respiratory systems, *IEEE Trans. Control Syst. Technol.*, **28** (2020), 163–171. doi: 10.1109/TCST.2018.2871002.
16. J. Reinders, R. Verkade, B. Hunnekens, N. van de Wouw, T. Oomen, Improving mechanical ventilation for patient care through repetitive control, in *21st IFAC World Congress*, (2020), 1441–1446. doi: 10.1016/j.ifacol.2020.12.1906.
17. H. Zhang, L. Cui, X. Zhang, Y. Luo, Data-driven robust approximate optimal tracking control for unknown general nonlinear systems using adaptive dynamic programming method, *IEEE Trans. Neural Netw.*, **22** (2011), 2226–2236. doi: 10.1109/TNN.2011.2168538.
18. Y. Pan, J. Wang, Model predictive control of unknown nonlinear dynamical systems based on recurrent neural networks, *IEEE Trans. Ind. Electron.*, **59** (2011), 3089–3101. doi: 10.1109/TIE.2011.2169636.
19. J. J. E. Slotine, W. Li, *Applied nonlinear control*, Englewood Cliffs, 1991.
20. H. K. Khalil, J. W. Grizzle, *Nonlinear systems*, Pearson Education Prentice hall, 2002.
21. A. Abrishamifar, A. Ahmad, M. Mohamadian, Fixed switching frequency sliding mode control for single-phase uni-polar inverters, *IEEE Trans. Power Electron.*, **27** (2011), 2507–2514. doi: 10.1109/TPEL.2011.2175249.
22. J. Zivcak, M. Kelemen, I. Virgala, P. Marcinko, P. Tuleja, M. Sukop, et al., An adaptive neuro-fuzzy control of pneumatic mechanical ventilator. *Actuators*, **10** (2021), 1–23. doi: 10.3390/act10030051.

23. Y. C. Hsu, H. A. Malki, Fuzzy variable structure control for MIMO systems, in *IEEE International Conference on Fuzzy Systems Proceedings, IEEE World Congress on Computational Intelligence.*, **1** (1998), 280–285. doi: 10.1109/FUZZY.1998.687498.
24. J. Schäublin, M. Derighetti, P. Feigenwinter, S. P. Felix, A. M. Zbinden, Fuzzy logic control of mechanical ventilation during anaesthesia, *Br. J. Anaesth.*, **77** (1996), 636–641. doi: 10.1093/bja/77.5.636.
25. H. Guler, F. Ata, Design of a fuzzy lab view-based mechanical ventilator, *Comput. syst. Sci. Eng.*, **29** (2014), 219–229.
26. D. Pelusi, Optimization of a fuzzy logic controller using genetic algorithms, in *IEEE 3rd International Conference on Intelligent HumanMachine Systems and Cybernetics*, **2** (2011), 143–146. doi: 10.1109/IHMSC.2011.105.
27. S. Kundu, D. R. Parhi, Reactive navigation of underwater mobile robot using ANFIS approach in a manifold manner, *Int. J. of Autom. Comput.*, **14** (2017), 307–320. doi: 10.1007/s11633-016-0983-5.
28. L. X. Wang, Design and analysis of fuzzy identifiers of nonlinear dynamic systems, *IEEE Trans. Automat. Contr.*, **40** (1995), 11–23. doi: 10.1109/9.362903.
29. M. Roopaei, M. Zolghadri, S. Meshksar, Enhanced adaptive fuzzy sliding mode control for uncertain nonlinear systems, *Commun. Nonlinear Sci. Numer. Simul.*, **14** (2009), 3670–3681. doi: 10.1016/j.cnsns.2009.01.029.
30. A. Saghafinia, H. W. Ping, M. N. Uddin, K. S. Gaeid, Adaptive fuzzy sliding-mode control into chattering-free IM drive, *IEEE Trans. Ind. Appl.*, **51** (2014), 692–701. doi: 10.1109/TIA.2014.2328711.
31. Y. Li, H. Wang, B. Zhao, K. Liu, Adaptive fuzzy sliding mode control for the probe soft landing on the asteroids with weak gravitational field, *Math. Probl. Eng.*, **2015** (2015), 1–8. doi: 10.1155/2015/582948.
32. A. Ishigame, T. Furukawa, S. Kawamoto, T. Taniguchi, Sliding mode controller design based on fuzzy inference for nonlinear systems (power systems), *IEEE Trans. Ind. Electron.*, **40** (1993), 64–70. doi: 10.1109/41.184822.
33. M. Roopaei, M. Z. Jahromi, Chattering-free fuzzy sliding mode control in mimo uncertain systems, *Nonlinear Anal. Theory Methods Appl.*, **71** (2009), 4430–4437. doi: 10.1016/j.na.2009.02.132.
34. H. S. Haghighi, A. H. Markazi, Chaos prediction and control in mems resonators, *Commun. Nonlinear Sci. Numer. Simul.*, **15** (2010), 3091–3099. doi: 10.1016/j.cnsns.2009.10.002.
35. O. Cerman, P. Hušek, Adaptive fuzzy sliding mode control for electro-hydraulic servo mechanism, *Expert Syst. Appl.*, **39** (2012), 10269–10277. doi: 10.1016/j.eswa.2012.02.172.
36. F. J. Lin, S. L. Chiu, Adaptive fuzzy sliding-mode control for PM synchronous servo motor drives, *IEE Proc. Control Theory Appl.*, **145** (1998), 63–72. doi: 10.1016/S0165-0114(03)00199-4.
37. S. Liu, L. Ding, Application of adaptive fuzzy sliding mode controller in PMSM servo system, in *IEEE International Conference on Computing*, **2** (2010), 95–98. doi: 10.1109/CCIE.2010.142.

38. N. Ullah, S. Wang, M. I. Khattak, M. Shafi, Fractional order adaptive fuzzy sliding mode controller for a position servo system subjected to aerodynamic loading and non-linearities, *Aerosp. Sci. Technol.*, **43** (2015), 381–387. doi: 10.1016/j.ast.2015.03.020.
39. N. Ullah, M. Asghar Ali, A. Ibeas, J. Herrera, Adaptive fractional order terminal sliding mode control of a doubly fed induction generator-based wind energy system, *IEEE Access*, **5** (2017), 21368–21381. doi: 10.1109/ACCESS.2017.2759579.
40. N. Ullah, A. Ibeas, M. Shafi, M. Ishfaq, M. Ali, Vaccination controllers for SEIR epidemic models based on fractional order dynamics, *Biomed. Signal Process. Control*, **38** (2017), 136–142. doi: 10.1016/j.bspc.2017.05.013.
41. N. Ullah, A. Ullah, A. Ibeas, J. Herrera, Improving the hardware complexity by exploiting the reduced dynamics-Based fractional order systems, *IEEE Access*, **5** (2017), 7714–7723. doi: 10.1109/ACCESS.2017.2700439.



AIMS Press

© 2022 the Author(s), licensee AIMS Press. This is an open access article distributed under the terms of the Creative Commons Attribution License (<http://creativecommons.org/licenses/by/4.0>)